

Ring Cleavage of Aziridines by Difluoroamine: Mechanistic Insights from *ab Initio* and DFT Study

Anbarasan Kalaiselvan,[†] Salai Cheettu Ammal,[‡] Ponnambalam Venuvanalingam,^{*,†} and Hiroshi Yamataka^{*,‡}

Department of Chemistry, Bharathidasan University, Tiruchirappalli-620 024, India, and Department of Chemistry, Rikkyo University, Nishi-Ikebukuro 3-34-1, Toshima-ku, Tokyo 171-8501, Japan

Received: December 6, 2004; In Final Form: April 1, 2005

cis-2,3-Dimethylaziridine reacts with difluoroamine to give the corresponding alkene and nitrogen with retention of configuration. We have carried out a DFT study of this reaction to clarify the reaction mechanism by considering a multistep reaction pathway with possible intermediacy of several three- and four-membered cyclic intermediates and transition states (TSs). The energetics of this reaction shows that the reaction takes place in four steps including a three-membered azamine intermediate. Both the energetics and the stereochemical outcome of this reaction rule out the formation of a four-membered diazetine intermediate during the reaction. Although the first N–N bond formation step is rate determining, the final step, asynchronous concerted cleavage of the azamine intermediate, explains the stereochemistry of this reaction. The asynchronous nature of the final step makes the reaction Woodward–Hoffmann allowed, as reported by Yamabe and Minato (*J. Phys. Chem. A* **2001**, *105*, 7281). Computations at HF and MP2 levels confirm the same trends in energetics. Single point energy computations at B3LYP, MP2, and QCISD levels with the 6-311++G(d,p) and cc-pVTZ basis sets show that the larger basis sets predict higher free energies of activation and less negative free energies of reaction. Intrinsic reaction coordinate (IRC) analyses reveal the asynchronous nature of the first and the last steps of the reaction. The deamination of *trans*-2,3-dimethylaziridine was shown to follow a course of reaction similar to that of the *cis* isomer.

Introduction

Aziridine, a three-membered heterocycle containing one nitrogen atom can be found in natural and synthetic compounds of biological interest.¹ Especially 2,3-disubstituted aziridines have widespread applications as versatile intermediates in synthetic organic chemistry.² Aziridines are susceptible to ring-opening reactions, and the driving force for this is the release of their ring strain. Generally, nonactivated aziridines undergo ring-opening reactions through either protonation, quarternization or through the formation of a Lewis acid adduct. With suitable choice of substituents on the carbon and nitrogen atoms, excellent stereo- and regiocontrol can be obtained in ring-opening reactions, which makes aziridines useful intermediates in organic chemistry.^{3,4}

Deamination⁵ can be done with several reagents such as 3-nitro-*N*-nitrosocarbazole, nitrosyl chloride, methyl nitrite, etc.,⁶ and in the majority of cases it yields alkenes with the retention of configuration. In a few cases,^{6a} alkene with inverted stereochemistry has been formed as a product and the reaction has been exploited in the interconversion of *cis*–*trans* isomers of alkenes. Retention or inversion of stereochemistry depends on the mechanism but there were only a few attempts^{7,8} to investigate the mechanism of this reaction. In this paper, we elucidate the mechanism of the deamination of aziridine by difluoroamine that results in the formation of an alkene with the retention of configuration.

Difluoroamine⁹ is an efficient and direct deaminating reagent, and it reacts with aziridine (**1**) to give alkene with 96%

stereospecificity.¹⁰ The reaction has been postulated to proceed through azamine (**2**) and collapse of this azamine results in the formation of alkene with evolution of nitrogen (Scheme 1). The mechanism of this reaction is not well understood and there is no firm experimental evidence for the proposed azamine intermediate. Moreover, it was claimed¹¹ that the elimination of nitrogen from a three-membered ring should be nonstereospecific. Such situations have stimulated us to study the reaction mechanism with the following questions in mind: (i) What is the overall mechanism of this reaction that leads to the retention of stereochemistry? (ii) Does the azamine intermediate indeed exist on the reaction pathway? (iii) Does the Woodward–Hoffmann rule control the stereochemistry of this reaction?

Computational Details

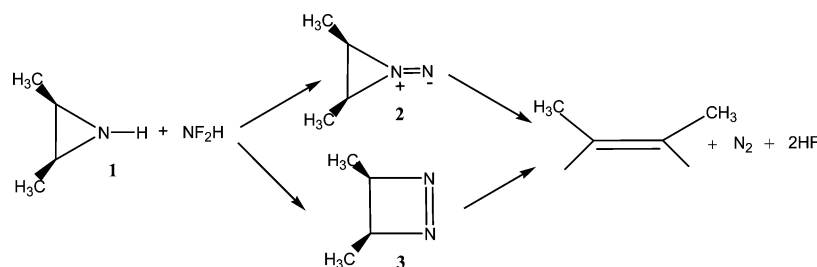
Geometries of species at all stationary points in the potential energy surface have been calculated with the B3LYP^{12,13} method using the 6-31G(d) basis set.¹⁴ Stationary points located have been characterized by computing vibrational frequencies; reactants, products, and intermediates have all real frequencies and the TSs have an imaginary frequency. The nature of the TSs have been confirmed by the mode of the imaginary frequency and by IRC calculations.¹⁵ Geometry optimizations have also been carried out at the HF¹⁶ and MP2 levels of theory¹⁷ with the 6-31G(d) basis set for the species on the lowest energy reaction pathway obtained at B3LYP/6-31G(d). Further single point energy calculations have been done at the B3LYP, MP2, and QCISD¹⁸ levels with larger basis sets 6-311++G(d,p) and cc-pVTZ on the B3LYP/6-31G(d) optimized geometries of the species on the lowest energy reaction pathway. All calculations have been performed with the Gaussian98 program.¹⁹ Free

* Author for correspondence. E-mail: venuvanalingam@yahoo.com.

[†] Bharathidasan University.

[‡] Rikkyo University.

SCHEME 1



energies of the species at the HF, B3LYP, and MP2 levels with the 6-31G(d) basis set have been calculated on the basis of their frequency calculations and for the larger basis sets they have been computed using thermal corrections data obtained at the B3LYP/6-31G(d) level. Intrinsic reaction coordinate analyses have been done for the transition structures obtained at the B3LYP level. Bond orders reported here are Wiberg²⁰ bond indices calculated by the natural bond orbital²¹ (NBO) program. From these bond orders, bond formation index BF_i and bond cleavage index BC_j are calculated as follows.^{8,22}

$$BF_i \text{ or } BC_j = \frac{BO_i^{\text{TS}} - BO_i^{\text{R}}}{BO_i^{\text{P}} - BO_i^{\text{R}}} \times 100 \quad (1)$$

BFC_{av} is the average percentage of all bond forming and cleaving indices of various species in the reaction step.

$$BFC_{\text{av}} = \frac{\sum_{ij} (BF_i + BC_j)}{n} \quad (2)$$

where n is the total number of bonds that undergo major changes during the reaction.

Results and Discussion

Possible Reaction Pathways. Aziridine undergoes deamination with difluoroamine to form alkene, as shown in Scheme 1. The reaction may proceed through either one of the two intermediates, azamine (**2**) that has been postulated by Bumgardner et al.⁹ or the diazetine intermediate (**3**). The detailed scheme of the reaction is given in Figure 1. Optimized geometries of some selected species in the reaction pathway are presented in Figure 2.

Difluoroamine approaches the aziridine nitrogen in two orientations, and in the first stage one molecule of HF is released with concomitant formation of an N–N bond. There are two possibilities for this: (i) the reactants form an initial complex, which yields **Int1** through **TS1**, and (ii) the reactants form **Int2a** through a spiro-type TS (**TS1a**). The former process resembles $S_{\text{N}}2$ -type reaction at the N atom,²³ which takes place together with the abstraction of the H atom on NHF_2 by the leaving F anion to give HF. There is another possibility that NHF_2 decomposes into NF and HF and the resultant nitrene NF attacks the aziridine to give **Int1**. This step has also been examined. The activation free energy for the process $\text{NHF}_2 \rightarrow \text{NF} + \text{HF}$ is found to be very high, $49.3 \text{ kcal}\cdot\text{mol}^{-1}$, and therefore this possibility has not been considered further.

Computations show that the $\text{N}_3\text{--N}_{15}$ bond in **Int1** can undergo a rotation about the newly formed $\text{N}_3\text{--N}_{15}$ bond through **TS2** to form **Int2**. This brings the fluorine atom close to the hydrogen on the aziridine nitrogen and then another molecule of HF is released through **TS3** to form **Int3** (**2**).

Alternatively, **Int1** can undergo a hydrogen migration from N_3 to N_{15} through **TS2a** to form **Int2a**. The H and F atoms attached to the exocyclic N atom in **Int2a** get closer and through **TS3a** one molecule of HF is released to form **Int3**. **Int3** referred to as azamine¹⁰ undergoes asynchronous concerted cycloreversion via **TS4** to finally yield *cis*-alkene and N_2 . In another branch line, **Int2** can undergo ring expansion through 1,2-carbon shift (**TS3b**) and forms **Int3b**. Subsequently, **Int3b** releases one molecule of HF through **TS4b** to form **Int4b**. **Int4b**, i.e., *cis*-3,4-dimethyldiazetine (**3**), also undergoes a concerted asynchronous cycloreversion to form *trans*-alkene and N_2 . It is interesting to note that, in the final step, both **Int3** and **Int4b** undergo cycloreversion but the stereochemistry is retained in the former and inverted in the latter.

Reaction Energetics. Frontier orbital energies of **1** and NHF_2 were calculated to be -0.37 eV (HOMO of **1**), 0.23 eV (LUMO of **1**), -0.51 eV (HOMO of NHF_2), and 0.21 eV (LUMO of NHF_2) at the MP2/6-31G(d) level of theory. These values show that the reaction is mainly controlled by the interaction between HOMO of **1** and LUMO of NHF_2 .

The free energy profile of the reaction at B3LYP/6-31G(d) is shown in Figure 3, in which the free energies of various TSs and intermediates are expressed with reference to the reactants. Difluoroamine reacts with aziridine through **TS1** or **TS1a** as mentioned above. The free energies of activation for these steps are found to be 42.6 and $56.9 \text{ kcal}\cdot\text{mol}^{-1}$, and the free energies of reaction are $+14.2$ and $-24.0 \text{ kcal}\cdot\text{mol}^{-1}$, respectively, at B3LYP/6-31G(d). The computed barriers suggest that the reaction passes through **TS1**. The barrier for this step is unrealistically high for a reaction that takes place smoothly, and inclusion of solvent effects may reduce the barrier drastically.

Int1 undergoes rotation about the $\text{N}_3\text{--N}_{15}$ single bond to form **Int2** with a low barrier of about $3.0 \text{ kcal}\cdot\text{mol}^{-1}$. Following this, the azamine intermediate (**Int3**, **2**) is formed from **Int2** through spiro-type **TS3**, and the barrier for this process is $22.3 \text{ kcal}\cdot\text{mol}^{-1}$. In this step, the $\text{N}_3\text{--N}_{15}$ double bond and $\text{H}_{14}\text{--F}_{16}$ single bond are formed and the $\text{N}_3\text{--H}_{14}$ and $\text{N}_{15}\text{--F}_{16}$ bonds are broken. The alternative step from **Int1** to **Int2a** through 1,2-proton migration from N_3 to N_{15} (**TS2a**) is a high-energy process ($40.5 \text{ kcal}\cdot\text{mol}^{-1}$). **Int2a** then leads to **Int3** through **TS3a** with a barrier of $18.4 \text{ kcal}\cdot\text{mol}^{-1}$. Free energy profiles of these processes indicate that the formation of **Int3** via **Int2** is the energetically favorable pathway. The azamine intermediate (**Int3**) undergoes asynchronous concerted cleavage of the ring with a low activation barrier of $8.1 \text{ kcal}\cdot\text{mol}^{-1}$.

Int2 may also undergo a 1,2-carbon shift to give **Int3b**, which is more stable than **Int3**, but the energy required for this step is high ($33.6 \text{ kcal}\cdot\text{mol}^{-1}$), probably because this TS (**TS3b**) has a [1,1,0] bicyclic structure. **Int3b** would give stable diazetine intermediate (**Int4b**, **3**), which then may decompose through an asynchronous concerted mode (**TS5b**) with the free energy of activation $43.9 \text{ kcal}\cdot\text{mol}^{-1}$ to form *trans*-alkene. The higher activation energy for the formation of **Int3b** as well as the

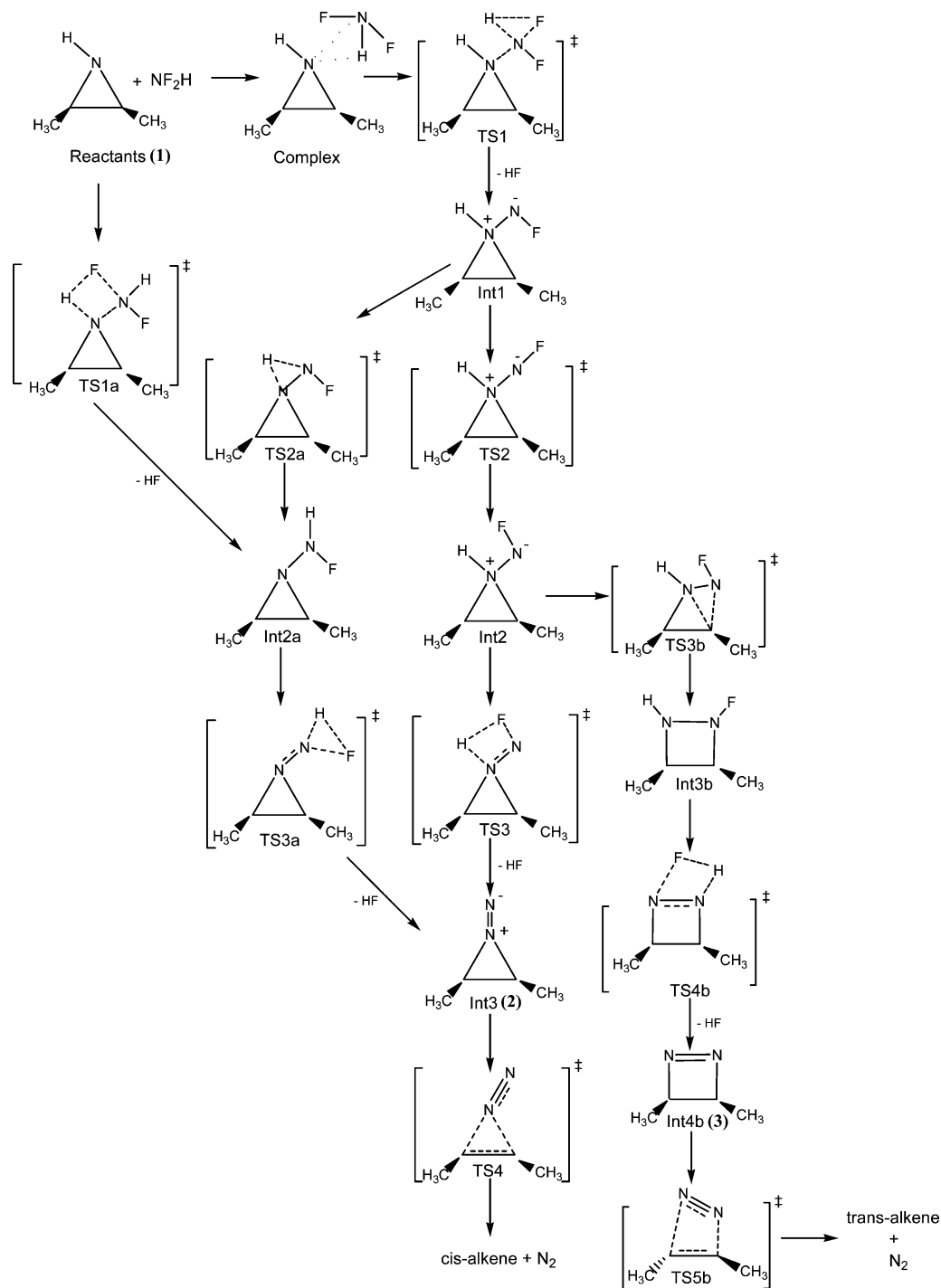


Figure 1. Reaction pathways for the deamination of *cis*-2,3-dimethylaziridine and NHF_2 .

stereochemistry of the product alkene can rule out the possible intermediacy of diazetine (**Int4b**) in this reaction. The possibility of TS4 and TS5b having a biradical character has been tested using UB3LYP calculations and stability of the wave function. The wave functions show RB3LYP \rightarrow UB3LYP stability, and this confirms that they are closed shell singlets and not biradicals. All these observations lead to the conclusion that the reaction takes place through the three-membered azamine intermediate (**Int3**) and not through the four-membered diazetine intermediate (**Int4b**). Thus, the reaction pathway is reactants \rightarrow complex \rightarrow **TS1** \rightarrow **Int1** \rightarrow **TS2** \rightarrow **Int2** \rightarrow **TS3** \rightarrow **Int3** \rightarrow **TS4** \rightarrow products. The formation of **Int3** from the reactants through the precursor **Int2a** is a high energy path. The most probable pathway is illustrated in Figure 4 with relative free

energies with respect to reactants at different levels of theory. The rate-determining step of the multistep reaction is the first step via **TS1**. The present results nicely explain the experimental observations that the whole reaction is taking place with 96% retention of stereochemistry; i.e., when HNF_2 is reacted with the *cis*-2,3-dimethylaziridine, *cis*-2-butene is the product, and when *trans*-2,3-dimethylaziridine is reacted, *trans*-2-butene is the product.

Geometrical Variation along the Lowest Energy Reaction Pathway. Geometries of species along the lowest energy pathway computed at B3LYP/6-31G(d) and MP2/6-31G(d) illustrated in Figure 2 are informative. The initial complex between the aziridine and NHF_2 is a true minimum on the potential energy surface with a weak $\text{N}_3\text{-H-N}_{15}$ hydrogen-

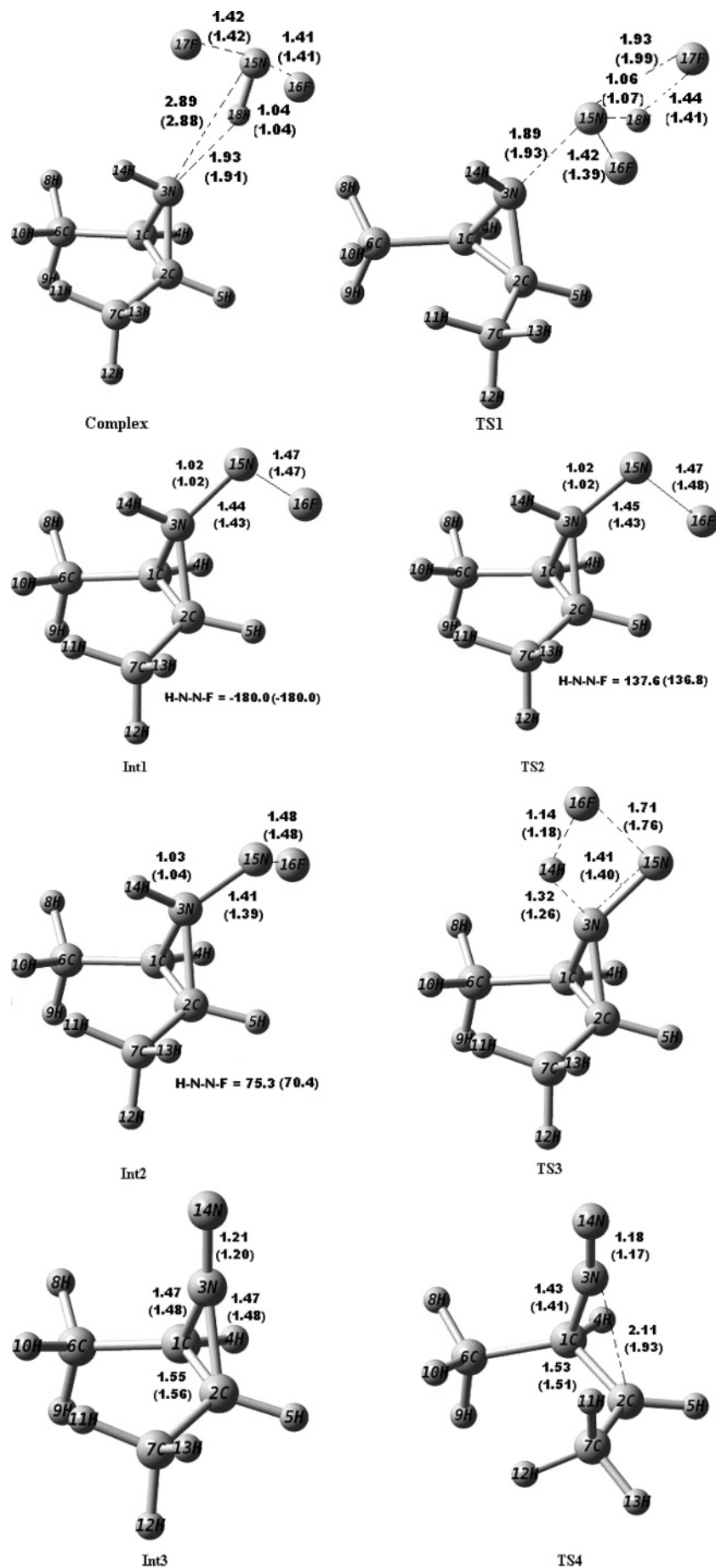


Figure 2. Optimized structures of complex, transition structures, and intermediates in the least energy pathway of deamination of aziridines with HNF₂ at MP2/6-31G(d) and (B3LYP/6-31G(d)) levels of theory. Distances are in Å, and dihedral angles are in degrees.

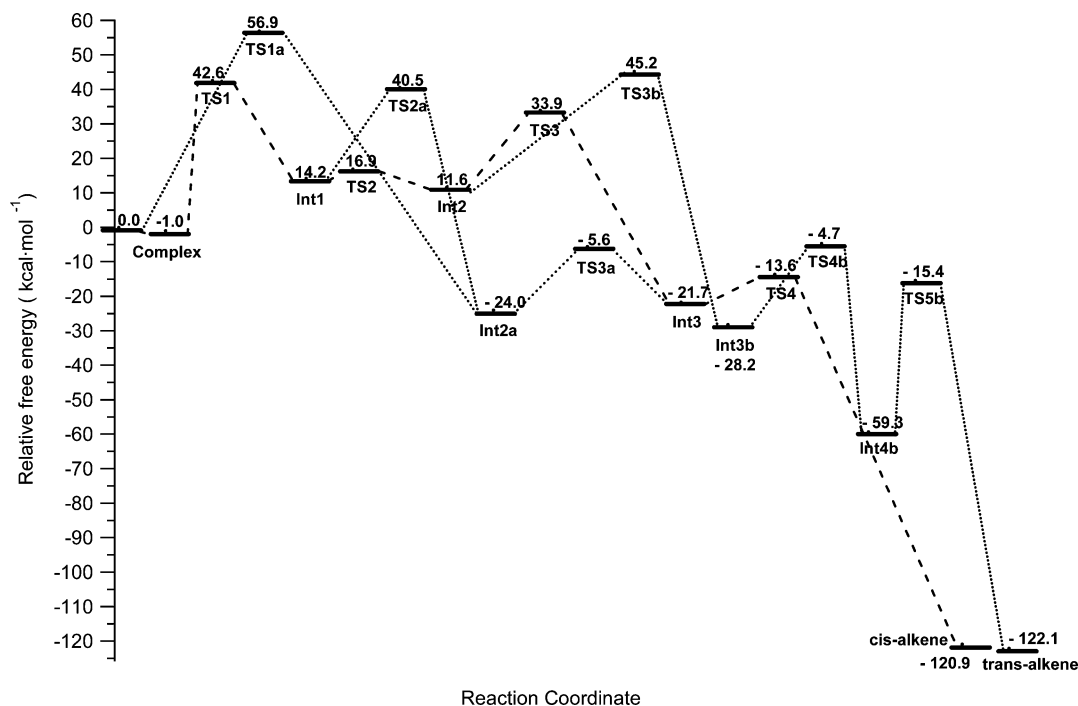


Figure 3. Schematic free energy profile for the deamination of *cis*-2,3-dimethylaziridine with NHf_2 at B3LYP/6-31G(d).

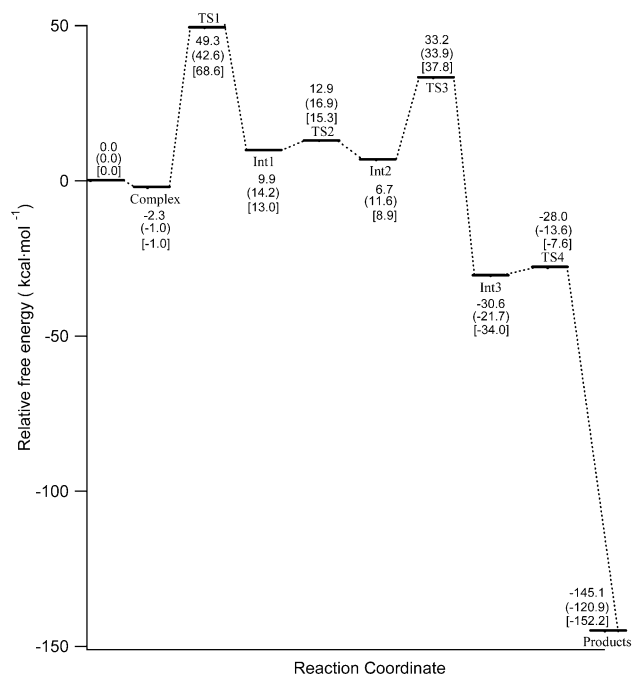


Figure 4. Schematic free energy profile for the least energy pathway with relative free energies of complex, transition states, intermediates and products with respect to reactants. Numbers are at MP2/6-31G(d), (B3LYP/6-31G(d)), and [HF/6-31G(d)].

bond interaction. Figure 5 shows the changes of selected bond lengths along IRC for the N–N bond formation step from the complex to **Int1**. The structural variations along IRC exhibit that two independent events occur in this step. One is an $\text{S}_{\text{N}}2$ -like displacement of F_{17} by N_3 at the nitrogen atom, N_{15} . Smooth variation of the two bond lengths and a nearly linear alignment of N_3 – N_{15} – F_{17} at **TS1** are characteristics of $\text{S}_{\text{N}}2$ displacement. The other one is the transfer of H_{18} from N_{15} to F_{17} . The hydrogen (H_{18}) on N_{15} is hydrogen-bonded to the aziridine nitrogen (N_3) in the initial complex. At the early stage of the reaction the hydrogen bond is cleaved and H_{18} starts to interact with F_{17} with the N_{15} – H_{18} bond nearly intact until **TS1**, and

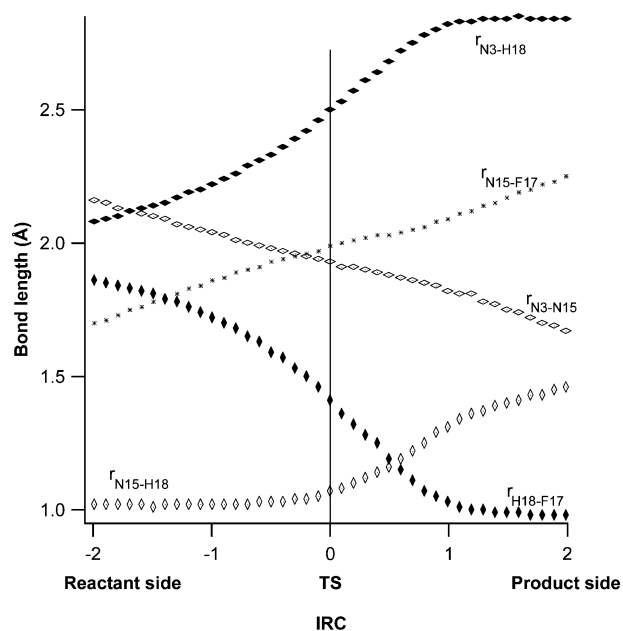


Figure 5. Changes in the lengths of various bonds along the IRC around **TS1** of aziridine deamination by HNF_2 at B3LYP/6-31G(d). The units of IRC are $\text{amu}^{-1/2} \text{ bohr}$.

then the proton transfer occurs from N_{15} to F_{17} after the **TS**. Thus, the step is a two-stage process with the N–N bond formation and the proton transfer occurring in different time scales.

On going from **Int1** to **Int2**, the dihedral angle $\angle \text{H}_{14}$ – N_3 – N_{15} – F_{16} changes from 180.0° in **Int1** through 137.6° in **TS2** to 75.3° in **Int2**. In **TS3**, further rotation around this bond takes place before liberation of an HF molecule. This **TS** has a distorted spiro structure where $\angle \text{H}_{14}$ – N_3 – C_2 – $\text{C}_1 = 130.4^\circ$ and $\angle \text{N}_{15}$ – N_3 – C_2 – $\text{C}_1 = -114.7^\circ$. The aziridine intermediate (**Int3**) formed from **TS3** undergoes ring opening in an asynchronous concerted fashion through **TS4**. This results in the formation of N_2 and alkene with the retention of configuration. In Figure 6 are shown the changes of selected bond lengths along IRC

TABLE 1: Relative Free Energies (kcal·mol⁻¹) of Complex, TSs, Intermediates and Product for the Deamination Reaction of *cis*-2,3-dimethylaziridine at Various Computational Methods with Respect to the Reactants

method	complex	TS1	Int1	TS2	Int2	TS3	Int3	TS4	products
HF/6-31G(d)	-1.0	68.6	13.0	15.3	8.9	37.8	-34.0	-7.6	-152.2
B3LYP/6-31G(d) ^a	-1.0	42.6	14.2	16.9	11.6	33.9	-21.7	-13.6	-120.9
	(-1.1)	(43.7)	(15.4)	(15.1)	(13.1)	(34.6)	(-20.9)	(-12.9)	(-120.1)
MP2/6-31G(d)	-2.3	49.3	9.9	12.9	6.7	33.2	-30.6	-28.0	-145.1
B3LYP/6-311++G (d,p) ^b	-0.7	35.1	1.8	3.4	-3.5	20.8	-46.5	-39.0	-146.6
MP2/6-311++G (d,p) ^b	-1.3	42.4	-1.2	1.1	-7.3	21.5	-53.2	-52.7	-166.5
QCISD/6-311++G (d,p) ^b	-0.5	44.2	0.4	2.8	-5.1	21.4	-50.6	-39.6	-161.0
B3LYP/cc-pVTZ ^b	-0.3	40.7	4.1	6.0	-0.4	22.4	-45.2	-39.1	-146.5
MP2/cc-pVTZ ^b	-0.5	48.4	4.8	7.0	-0.3	26.8	-43.3	-44.1	-156.4
QCISD/cc-pVTZ ^b	0.4	50.0	5.9	8.3	1.3	26.2	-42.3	-31.9	-153.3

^a Values given in parentheses correspond to the deamination of *trans*-2,3-dimethylaziridine computed at B3LYP/6-31G(d). ^b Values obtained with single point calculations on the specified level on the B3LYP/6-31G(d) geometries.

TABLE 2: Wiberg Bond Order Analysis of Deamination of *cis*-Aziridines with HNF₂ at B3LYP/6-31G(d)

species	BF _i				BC _j						BFC _{av}
	C ₁ -C ₂	N ₃ -N ₁₅	H ₁₈ -F ₁₇	H ₁₄ -F ₁₆	C ₁ -N ₃	C ₂ -N ₃	N ₃ -H ₁₄	N ₁₅ -F ₁₆	N ₁₅ -F ₁₇	N ₁₅ -H ₁₈	
reactants	0.0	0.0	0.0	0.0	0.0	0.0	0.0	0.0	0.0	0.0	0.0
complex	0.0	0.7	0.0	0.0	1.0	1.0	2.4	0.0	2.1	9.4	1.7
TS1	0.0	15.2	21.1	0.0	3.1	3.1	6.0	0.0	52.1	22.4	12.3
Int1	0.0	33.7	100.0	0.0	12.5	12.5	9.5	9.6	100.0	100.0	37.8
TS2	0.0	34.0	100.0	0.0	17.7	9.4	9.5	8.3	100.0	100.0	37.9
Int2	0.0	35.0	100.0	0.0	9.4	16.7	13.1	9.6	100.0	100.0	38.5
TS3	0.0	36.3	100.0	46.5	8.3	8.3	57.1	39.4	100.0	100.0	49.6
Int3	0.0	65.4	100.0	100.0	11.5	11.5	100.0	100.0	100.0	100.0	68.8
TS4	0.0	75.3	100.0	100.0	0.0	52.1	100.0	100.0	100.0	100.0	72.7
products	100.0	100.0	100.0	100.0	100.0	100.0	100.0	100.0	100.0	100.0	100.0

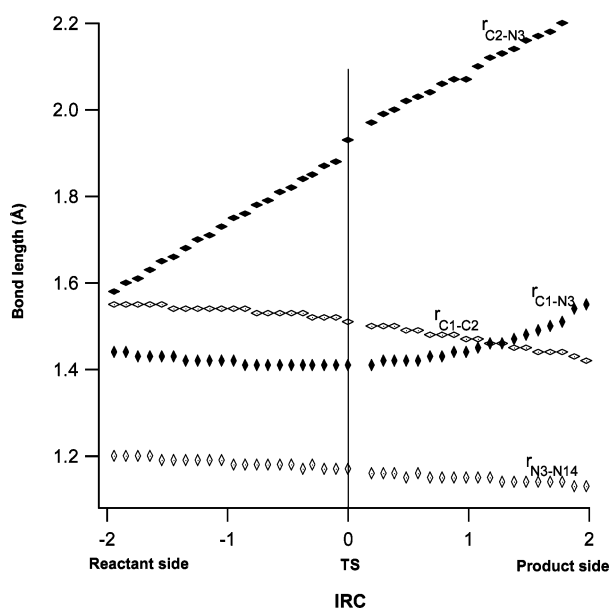


Figure 6. Changes in the lengths of various bonds along the IRC around TS4 of aziridine deamination by HNF₂ at B3LYP/6-31G(d). The units of IRC are amu^{-1/2} bohr.

for the final alkene-forming step. It is clearly seen that the cleavage of the C₂-N₃ bond comes ahead of that of the C₁-N₃ bond. Thus, the step is a two-stage reaction in terms of the change in bonding and hence in electronic structure.

Yamabe and Minato have previously discussed the mechanism of N₂ extrusion from azamine and diazetine systems and have pointed out that both of them undergo cycloreversion through asynchronous concerted mechanism.⁷ They have demonstrated that Jahn-Teller distortion occurs in the TSs and that after symmetry lowering azamine decomposition becomes Woodward-Hoffmann allowed whereas diazetine reaction does not follow the symmetry conservation rule. Our observation that azamine reacts in an asynchronous concerted manner with

retention of configuration agrees with the symmetry lowering argument reported by the above authors.

Effect of Various Methods and Basis Sets. Table 1 lists the relative free energies of the complex, TSs, the intermediates, and the products at different computational methods. It is clear that all these methods and basis sets predict the first step being rate determining. Therefore, it is worthwhile to compare the effects of various levels and basis sets on the free energy of activation for the first step. With the 6-31G(d) basis set, B3LYP predicts the lowest activation energy, whereas the HF value is the highest. With 6-311++G(d,p) and cc-pVTZ basis sets, B3LYP values are lower compared to QCISD and MP2 values. The energetics for the deamination of *trans*-2,3-dimethylaziridine at the B3LYP/6-31G(d) level listed in Table 1 reveals that the mechanism of *trans*-2,3-dimethylaziridine is basically the same as the *cis*-isomer.

Bond Order Analysis. Weak bond indices in Table 2 for the complex show the weak nature of the interaction between the reacting species. No major changes in bond indices are observed between **Int1**, **TS2**, and **Int2**, because the bond rotation is the major reaction coordinate in this step. The asynchronous nature of the concerted cycloreversion from **Int3** to the final product alkene and N₂ is clearly seen in the bond indices; the bond order is much larger for C₂-N₃ than for C₁-N₃ at **TS4**. The gradual increase in BFC_{av} from the reactants to the products shows the progress of the reaction quantitatively. In the whole reaction, the three-membered ring is intact till the last step and in the final step it cleaves concertedly. This does not allow the C₁-C₂ bond of the ring to undergo any rotation and is responsible for the retention of the stereochemistry.

Conclusions

Deamination of *cis*- and *trans*-2,3-dimethylaziridine with difluoroamine has been investigated by DFT calculations at the B3LYP/6-31G(d) level. Pathways with possible intermediacy of several three- and four-membered cyclic intermediates and

TSs have been considered. Analysis of the energies of this reaction has revealed that (i) the reaction involves four steps with initial formation of a complex, (ii) the reacting system eliminates two molecules of HF in two subsequent steps resulting in the formation of azamine intermediate, as suggested by earlier experimental reports, and (iii) the azamine intermediate cleaves in a concerted asynchronous way to form the corresponding alkene with retention of stereochemistry. The asynchronous nature of the step makes the reaction Woodward–Hoffmann allowed, as reported by Yamabe and Minato. The formation of the diazetine intermediate has been ruled out on the basis of the energetics and also on the observation that this intermediate inverts the stereochemistry of the reaction. The first step of the reaction is found to be rate determining, and the reaction is highly exothermic. The possible involvement of nitrene in the first step was eliminated in view of very high free energy of activation for the process $\text{NHF}_2 \rightarrow \text{NF} + \text{HF}$. Computations at HF and MP2 levels with the 6-31G(d) basis set also bring out the same conclusions. Single point energy computations at the B3LYP, MP2, and QCISD levels with the 6-311++G(d,p) and cc-pVTZ basis sets on the B3LYP/6-31G(d) geometries also confirm that the first step is rate determining. Geometrical changes in the first and last steps through IRC analysis and bond order analysis reveal that these are two-stage single step reactions.

Acknowledgment. The financial assistance from UGC, India, through Major Research Grant No. F:12-30/2002 (SR-1) (May 21, 2002) is gratefully acknowledged. S.C.A. and H.Y. thank the Research Center for Computational Science, Okazaki National Research Institute, for computing time. The study was partly supported by the Grant-in-Aid for Scientific Research from the Ministry of Education, Culture, Sports, Science, and Technology, Japan.

Supporting Information Available: HF/6-31G(d), B3LYP/6-31G(d), and MP2/6-31G(d) optimized Cartesian coordinates of all the species in the low lying path and B3LYP/6-31G(d) optimized Cartesian coordinates and structures of all species in the high lying paths. This material is available free of charge via the Internet at <http://pubs.acs.org>.

References and Notes

- (1) Mimura, N.; Miwa, Y.; Ibuka, T.; Yamamoto, Y. *J. Org. Chem.* **2002**, *67*, 5796.
- (2) (a) Moran, E. J.; Tellew, J. E.; Zhao, Z.; Armstrong, R. W. *J. Org. Chem.* **1993**, *58*, 7096. (b) Ahman, J.; Javevang, T.; Somfai, P. *J. Org. Chem.* **1996**, *61*, 8148.
- (3) Tanner, D. *Angew. Chem., Int. Ed. Engl.* **1994**, *33*, 559.
- (4) Sonnet, P. E. *Tetrahedron* **1980**, *36*, 557.
- (5) Carlson, R. M.; Lee, S. Y. *Tetrahedron Lett.* **1969**, *45*, 4001.
- (6) (a) Clark, R. D.; Helmkamp, G. K. *J. Org. Chem.* **1964**, *29*, 1316. (b) Carpino, L. A.; Kirkley, R. K. *J. Am. Chem. Soc.* **1970**, *92*, 1784.
- (7) Yamabe, S.; Minato, T. *J. Phys. Chem. A* **2001**, *105*, 7281.
- (8) Kalaiselvan, A.; Venuvanalingam, P.; Poater, J.; Sola, M. *Int. J. Quantum Chem.* **2005**, *102* (2), 139.
- (9) Bumgardner, C. L.; Martin, K. J.; Freeman, J. P. *J. Am. Chem. Soc.* **1963**, *85*, 97.
- (10) Freeman, J. P.; Graham, W. H. *J. Am. Chem. Soc.* **1967**, *89*, 1761.
- (11) Hoffmann, R.; Woodard, R. B. *Abstracts, 150th National Meeting of the American Chemical Society*, Atlantic City, NJ, Sept 1965; American Chemical Society: Washington, DC, p 85.
- (12) Becke, A. D. *J. Chem. Phys.* **1993**, *98*, 5648.
- (13) Lee, C.; Yang, W.; Parr, R. G. *Phys. Rev. B* **1988**, *37*, 785.
- (14) Frisch, M. J.; Pople, J. A.; Binkley, J. S. *J. Chem. Phys.* **1984**, *80*, 3265.
- (15) Fukui, K. *J. Phys. Chem.* **1970**, *74*, 4161. Ishida, K.; Morokuma, K.; Komornicki, A. *J. Chem. Phys.* **1977**, *66*, 2153.
- (16) Roothaan, C. C. J. *Rev. Mod. Phys.* **1951**, *23*, 69.
- (17) Curtiss, L. A.; Redfern, P. C.; Raghavachari, K.; Rasstolov, V.; Pople, J. A. *J. Chem. Phys.* **1999**, *110*, 4703.
- (18) Pople, J. A.; Gordon, M. H.; Raghavachari, K. *J. Chem. Phys.* **1987**, *87*, 5968.
- (19) Frisch, M. J.; Trucks, G. W.; Schlegel, H. B.; Scuseria, G. E.; Robb, M. A.; Cheeseman, J. R.; Zakrzewski, V. G.; Montgomery, J. A.; Stratmann, R. E.; Burant, J. C.; Dapprich, S.; Millam, J. M.; Daniels, A. D.; Kudin, K. N.; Strain, M. C.; Farkas, O.; Tomasi, J.; Barone, V.; Cossi, M.; Cammi, R.; Mennucci, B.; Pomelli, C.; Adamo, C.; Clifford, S.; Ochterski, J.; Petersson, G. A.; Ayala, P. Y.; Cui, Q.; Morokuma, K.; Malick, D. K.; Rabuck, A. D.; Raghavachari, K.; Foresman, J. B.; Cioslowski, J.; Ortiz, J. V.; Stefanov, B. B.; Liu, G.; Liashenko, A.; Piskorz, P.; Komaromi, I.; Gomperts, R.; Matin, R. L.; Fox, D. J.; Keith, T.; Al-Laham, M. A.; Peng, C. Y.; Nanayakkara, A.; Gonzalez, C.; Challacombe, M.; Gill, P. M. W.; Johnson, B. G.; Chen, W.; Wong, M. W.; Andres, L.; Head-Gordon, M.; Replogle, E. S.; Pople, J. A. *Gaussian 98*, revision A.9; Gaussian Inc.: Pittsburgh, PA, 1998.
- (20) Wiberg, K. *Tetrahedron* **1968**, *24*, 1083.
- (21) (a) Reed, A. E.; Curtiss, L. A.; Weinhold, F. *Chem. Rev.* **1988**, *88*, 889. (b) Foster, J. P.; Weinhold, F. *J. Am. Chem. Soc.* **1980**, *102*, 7211.
- (22) (a) Manoharan, M.; Venuvanalingam, P. *J. Mol. Struct. (THEO-CHEM)* **1997**, *394*, 41. (b) Manoharan, M.; Venuvanalingam, P. *J. Chem. Soc., Perkin Trans. 2* **1996**, 1423. (c) Manoharan, M.; Venuvanalingam, P. *J. Chem. Soc., Perkin Trans. 2* **1997**, 1799.
- (23) (a) Yi, R.; Basch, H.; Hoz, S. *J. Org. Chem.* **2002**, *67*, 5891. (b) Yi, R.; Chu, S. Y. *J. Phys. Chem. A* **2004**, *108*, 7079. (c) Glukhovtsev, M. N.; Pross, A.; Radom, L. *J. Am. Chem. Soc.* **1995**, *117*, 9012.